Editors' Suggestion

Rare thermal bubbles at the many-body localization transition from the Fock space point of view

Giuseppe De Tomasi,[1] Ivan M. Khaymovich,[2,3] Frank Pollmann,[4] and Simone Warzel[5]
[1]*T.C.M. Group, Cavendish Laboratory, J.J. Thomson Avenue, Cambridge CB3 0HE, United Kingdom*
[2]*Max-Planck-Institut für Physik komplexer Systeme, Nöthnitzer Straße 38, 01187 Dresden, Germany*
[3]*Institute for Physics of Microstructures, Russian Academy of Sciences, 603950 Nizhny Novgorod, GSP-105, Russia*
[4]*Department of Physics, Technische Universität München, 85747 Garching, Germany*
[5]*Department of Mathematics, Technische Universität München, 85747 Garching, Germany*

(Received 10 January 2021; revised 7 June 2021; accepted 11 June 2021; published 6 July 2021)

In this paper we study the many-body localization (MBL) transition and relate it to the eigenstate structure in the Fock space. Besides the standard entanglement and multifractal probes, we introduce the radial probability distribution of eigenstate coefficients with respect to the Hamming distance in the Fock space and relate the cumulants of this distribution to the properties of the quasilocal integrals of motion in the MBL phase. We demonstrate nonself-averaging property of the many-body fractal dimension D_q and directly relate it to the jump of D_q as well as of the localization length of the integrals of motion at the MBL transition. We provide an example of the continuous many-body transition confirming the above relation via the self-averaging of D_q in the whole range of parameters. Introducing a simple toy model, which hosts ergodic thermal bubbles, we give analytical evidences both in standard probes and in terms of newly introduced radial probability distribution that the MBL transition in the Fock space is consistent with the avalanche mechanism for delocalization, i.e., the Kosterlitz-Thouless scenario. Thus, we show that the MBL transition can been seen as a transition between ergodic states to nonergodic extended states and put the upper bound for the disorder scaling for the genuine Anderson localization transition with respect to the noninteracting case.

DOI: 10.1103/PhysRevB.104.024202

I. INTRODUCTION

Understanding the emergence of ergodicity in closed quantum many-body systems is an active front of research [1–6]. Generic interacting systems are expected to thermalize under their own quantum dynamics. Nevertheless, thermalization may fail if the system is subjected to strongly quenched disorder, giving arise to a new phase of matter dubbed as many-body localized (MBL) [7–13].

The MBL phase is best understood in terms of an emergent form of integrability, which is characterized by the existence of an extensive set of quasilocal conserved quantities, which strongly hinder thermalization in the system [14–16]. As a consequence, the system has Poisson level statistic, area-law entanglement, and the partial local structure of the initial state is maintained under the evolution [9,10,17]. Instead at weak disorder, the system is in an ergodic phase, meaning that eigenstate thermalization hypothesis [1,2,4,6] (ETH) holds, and therefore local observable thermalize. This implies that the system is fully described in terms of few macroscopic conserved quantities, i.e., energy and/or particles number.

A quantum phase transition, referred to as MBL transition [9], is believed to separate an ergodic phase from an MBL one. The MBL transition is a dynamical phase transition, meaning that it occurs at the level of individual eigenstates even at high energy density. In the last decade an enormous effort, both numerically and theoretically [7,17–25], has been made to understand the nature of this transition. Nevertheless, only little is known about the MBL transition. Numerically, the critical exponents associated with a putative second-order

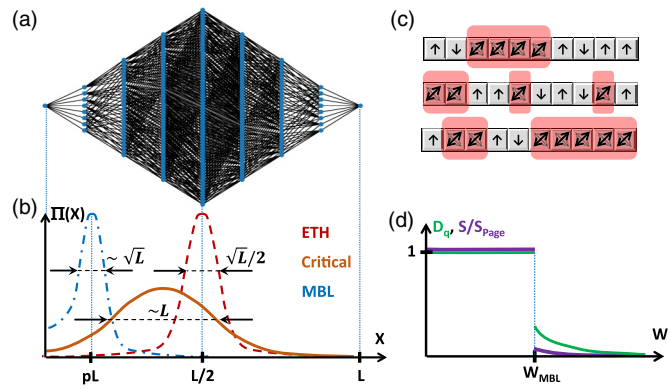

FIG. 1. (a) Representation in the Fock space (hypercube) of the many-body Hamiltonian $\widehat{H}_{\rm MBL}$ vs the Hamming distance. The blue nodes represent the basis vectors, which are connected by $\widehat{H}_{\rm MBL}$. (b) Cartoon picture of the radial probability distribution $\Pi(x)$ of an eigenstate with respect to the same Hamming distance x as in the panel (a) in the Fock space from the maximum of the wave function. In the ergodic/ETH phase $\Pi(x) = \frac{1}{2^L}\binom{L}{x}$ with the maximum at $x = L/2$, where most of the sites in the Fock space are. In the MBL phase, $\Pi(x)$ is skewed on the left with the width $\sim\sqrt{L}$. At the critical point, $\Pi(x)$ is much broader and fluctuations are extensive in L. (c) Pictorial representation of the rare thermal bubbles (in red), lengths of which are highly fluctuating at the critical point. The spins in red regions are entangled to each other (shown by many arrows), while the spins away from these regions are considered to be frozen (up or down). (d) Sketch of the jump of the entanglement entropy S normalized by its ergodic value $S_{\rm Page}$ and the fractal dimension D_q across the MBL transition.

type of the transition, are in disagreement with generic bounds [17,26]. This incongruence could be due to the fact that the system sizes analyzed using exact diagonalization techniques are too small to capture the true asymptotic behavior.

Very recently, several theoretical works have doubted the underline assumptions that the transition is of the second order. Phenomenological renormalization group studies suggest that the MBL transition could be of a Kosterlitz-Thouless (KT) type [27–32]. This possible scenario is properly predicted by a possible delocalization mechanism called avalanche theory, which takes into account nonperturbative effects possibly destabilizing the MBL phase [27,28]. Strictly speaking, the theory states that the presence of thermal bubbles in the system due to unavoidable entropic arguments is enough to destabilize the MBL phase if the localization length $\xi_{\rm loc}$ settled by the disorder strength exceeds a finite critical length. An immediate consequence of this mechanism is that the MBL is characterized not by the *divergence* of the correlation length, as one expects from the ordinary second-order transition, but by a *finite jump* of the inverse localization length across the transition [28,30].

A complementary interesting perspective is to characterize MBL systems in the Fock space, see Fig. 1(a) for a pictorial representation. This paradigm is based on the original idea of mapping a disordered quantum dot to a localization problem in the Fock space [33], which has been developed further recently [34]. This has been used to provide evidence of the existence of an MBL transition by Basko, Aleiner, and Altshuler in their seminal work [7]. Ergodicity is then defined through the fractal dimensions D_q, which quantify the spread of a state in the Fock space [35]. Ergodic states at infinite temperatures are believed to behave like random vectors [36,37], therefore they are spread homogeneously over the entire Fock space and $D_q = 1$. Instead, nonergodic states cover only a vanishing fraction of the Fock space, $0 \leqslant D_q < 1$. A genuine localization in the Fock space requires $D_q = 0$, though due to the many-body nature of the problem is never reached at finite disorder [17,38–43]. Thus, the MBL transition can be seen as an ergodic to nonergodic transition in the Fock space, with $D_q = 1$ in the ETH phase and $D_q < 1$ in the MBL phase.

In a recent paper [40], the behavior of D_q for a certain MBL model has been inspected using extensive numerical calculations. The MBL transition was found to be characterized by a jump in the fractal dimensions D_q at the critical point. The aforementioned investigations lead to the indication of the existence of an MBL transition. However, a clear connection between the above two viewpoints is still missing.

In this work, we focus on the existence of the above jump in the fractal dimensions and on its connection to the avalanche theory, i.e., to the KT-type transition from another perspective. Based on the breakdown of self-averaging for D_q at the transition and on the recently developed relation of D_q to the entanglement entropy [44], we show that the MBL transition is consistent with the jump of D_q from $D_q = 1$ to $D_q < 1/2$. The latter statement of the jump to $D_q < 1/2$ is an observation based on numerics [40], which is in agreement with the general bounds of the entanglement entropy in Ref. [44]. In addition, we focus on the radial distribution of a many-body eigenstate in the Fock space around its maximum, relate it to the behavior of local integrals of motion [45], and, thus, confirm the consistency of the KT scenario [28,30] for the MBL transition, see Fig. 1 for an overall picture.

This paper is organized as follows. In Sec. II we introduce the model and the indicators that we inspected numerically. In particular, we study the inverse participation ratio of eigenstate coefficients in the Fock space, from which we extract the fractal dimensions and the radial probability of eigenstate coefficients. Section III represents the numerical results concerning the fractal dimensions and the radial probability distribution. In Sec. IV we show our analytical considerations, which underline the connection between the avalanche theory and the observed jump in the fractal dimensions.

In Sec. V, we provide an example of an noninteracting model with many-body filling, which is known to have a delocalization-localization transition and characterized by a diverging localization length at this transition. We show the main difference of this model from the MBL transition, which is believed to have a discontinuity in the inverse localization length. Finally, we draw our conclusions and outlooks in Sec. VI.

II. MODEL AND METHODS

We study the random quantum Ising model [45] with the Hamiltonian

$$\widehat{H}_{\rm MBL} = \sum_i^L \widehat{\sigma}_i^x + \sum_i^L h_i \widehat{\sigma}_i^z + V \sum_i^L J_i \widehat{\sigma}_i^z \widehat{\sigma}_{i+1}^z, \qquad (1)$$

of a spin chain of the length L with periodic boundary conditions and the Pauli operators at site i given by σ_i^α for $\alpha \in \{x, y, z\}$. h_i and J_i are independent random variables uniformly distributed in $[-W, W]$ and $[0.8, 1.2]$, respectively. W is the disorder and $V = 1$ is the interaction strengths.

In Ref. [45] under mild assumptions of the absence on energy level attraction the existence of the MBL phase has been established for sufficiently large, but finite W. Moreover, numerically the critical disorder strength of the MBL transition has been identified as $W_c \approx 3.5$ [46].

In the noninteracting limit of $V = 0$ the Hamiltonian, Eq. (1), represents a system of uncoupled spins, which is trivially localized in the sense that all eigenstates are product states. In this limiting case, the Hamiltonian can be expressed $\widehat{H} = \sum_i \epsilon_i \widehat{\tau}_i^z$ through its integrals of motion $\widehat{\tau}_i^z = \widehat{U}_i \widehat{\sigma}_i^z \widehat{U}_i^\dagger$ obtained from the original spins by a single-spin rotation

$$\widehat{U}_i = \begin{pmatrix} \cos\frac{\theta_i}{2} & -\sin\frac{\theta_i}{2} \\ \sin\frac{\theta_i}{2} & \cos\frac{\theta_i}{2} \end{pmatrix}, \qquad (2)$$

with $\sin\theta_i = 1/\sqrt{1+h_i^2}$ and the single-spin energies $\epsilon_i = \sqrt{1+h_i^2}$. This example directly shows that the eigenstates $\{|\underline{\tau}^z\rangle\}$ of $\widehat{H}_{\rm MBL}$ with $V = 0$ are adiabatically connected to the σ_z-basis product states $|\underline{\sigma}^z\rangle = \otimes_i |\sigma_i^z\rangle$ with $\sigma_i^z \in \{-1, 1\}$ through local rotations $\prod_i \widehat{U}_i |\underline{\sigma}^z\rangle = |\underline{\tau}^z\rangle$. In Ref. [45] it has been shown that for $V \neq 0$ and sufficiently large W, $\widehat{H}_{\rm MBL}$ can

still be diagonalized via a sequence of local rotations, which adiabatically connect the eigenstates to the product states in the σ_z basis.

Another useful perspective of the model Eq. (1) is to consider it as an Anderson model on the Fock space. For this, one can rewrite the Hamiltonian in the σ_z basis and associate the first term in Eq. (1) to the hopping and the rest to the on-site correlated disorder on a L-dimensional hypercube,

$$\widehat{H}_{\rm MBL} = \sum_{\underline{\sigma}^z \sim \underline{\sigma}'^z} |\underline{\sigma}^z\rangle \langle \underline{\sigma}'^z| + \sum_{\underline{\sigma}^z} E_{\underline{\sigma}^z} |\underline{\sigma}^z\rangle \langle \underline{\sigma}^z| \ , \tag{3}$$

where $|\underline{\sigma}^z\rangle$ stands for the configuration given by the vector $\underline{\sigma}^z$ of L values $\sigma_i^z = \{+1, -1\}$, while $\underline{\sigma}^z \sim \underline{\sigma}'^z$ means that the corresponding vectors differ by a single spin flip. In this representation the first sum in $\widehat{H}_{\rm MBL}$ can be understood as the Laplace operator on the hypercube as it connects spins configurations, which differ by one spin flip, and $E_{\underline{\sigma}^z} = \sum_i h_i \sigma_i^z + \sum_i J_i \sigma_i^z \sigma_{i+1}^z$ are the diagonal energies. It is important to note that the 2^L diagonal entries $\{E_{\underline{\sigma}^z}\}$ are strongly correlated random variables since they are constructed only from $2L$ random variables $\{h_i\}$ and $\{J_i\}$. Indeed, even though typical fluctuations of the entries scales as $\sqrt{L}$, their level spacings $E_{\underline{\sigma}^z} - E_{\underline{\sigma}'^z}$ are $O(1)$ if $\underline{\sigma}^z \sim \underline{\sigma}'^z$.

This model should be distinguished from the quantum random energy model (QREM) [47–49] for which the first two terms in (1) or equivalently the last term in (3) are replaced by z-diagonal entries $\{E_{\underline{\sigma}^z}\}$, which are independent identically distributed Gaussian random variables $\mathcal{N}(0, W^2 L)$. The QREM has an Anderson transition at $W_c \sim \sqrt{L \log L}$ (cf. Eq. 10.15 [50]) for which $D_q = 0$.

Ergodic properties of an eigenstate $|E\rangle$ of $\widehat{H}_{\rm MBL}$ in Eq. (3) can be quantified using the generalized inverse participation ratio (IPR_q)

$$\mathrm{IPR}_q = \sum_{\underline{\sigma}^z}^{2^L} |\langle \underline{\sigma}^z | E\rangle|^{2q}, \tag{4}$$

which quantifies the spread of $|E\rangle$ over the Fock space. Through the IPR_q the fractal dimensions are defined as

$$D_q = \frac{\log \mathrm{IPR}_q}{(1-q) L \log 2}. \tag{5}$$

Ergodic states at infinite temperature are characterized by $D_q = 1$ since they extend over the entire Fock space $|\langle \underline{\sigma}^z | E\rangle|^2 \sim 1/2^L$. In general, $0 < D_q < 1$ corresponds to the nonergodic (or multifractal) states, while the extreme case $D_q = 0$ refers to the localized ones.

For a model similar to $\widehat{H}_{\rm MBL}$ considered in [40] it has been shown that in the ergodic phase ($W < W_c$) mid-spectrum eigenstates show $D_q = 1$. Instead, in the MBL phase $D_q < 1$ and the fractal dimension experiences a jump at the critical point. It is important to point out that due to the many-body nature of the wave functions $D_q > 0$ [17,39,40,43] for any finite values of W, even deeply in the MBL phase.

The last observation is closely related to the tensor product structure of the Fock space and the Hamiltonian's local structure. Indeed, in the noninteracting limit ($V = 0$) spins are decoupled, i.e., $\mathrm{IPR}_q^{V=0} = \prod_i^L \mathrm{IPR}_q^{(i)}$ and the one-site $\mathrm{IPR}_q^{(i)}$ is smaller than one

$$\mathrm{IPR}_q^{(i)} = \sum_{\sigma_z \in \{\uparrow,\downarrow\}} |\langle \sigma_z | \tau_i^z \rangle|^{2q} < 1 \ . \tag{6}$$

As a consequence, $\mathrm{IPR}_q^{V=0} \sim 2^{-(q-1)\overline{D_q^0} L + \mathcal{O}(\sqrt{L})}$ decays exponentially with the strictly positive exponent

$$\overline{D_q^0} = \frac{\overline{\log \mathrm{IPR}_q^{(i)}}}{(1-q)\log 2} > 0 \ . \tag{7}$$

This fractal exponent is self-averaging as it is the sum of independent random variables and has fluctuations $\mathcal{O}(1/\sqrt{L})$ shown above in the exponent of the IPR [51]. At this point, it is important to appreciate the difference between the MBL phase of $\widehat{H}_{\rm MBL}$ and the localized phase for the QREM. The first one is characterized by a strictly positive fractal dimension, while in the second one $D_q = 0$.

For a better understanding of the ergodicity properties from the Fock space point of view, we define the radial probability distribution $\Pi(x)$ [52] of an eigenstate $|E\rangle$ as

$$\Pi(x) = \overline{\sum_{d(\underline{\sigma}^z, \underline{\sigma}_0^z) = x} |\langle \underline{\sigma}^z | E\rangle|^2}, \tag{8}$$

where the sum runs over the $\binom{L}{x}$ spin states $\{|\underline{\sigma}^z\rangle\}$, which differ by x flips [i.e., at the Hamming distance $d(\underline{\sigma}^z, \underline{\sigma}_0^z) = x$] from $|\underline{\sigma}_0^z\rangle$, which corresponds to the maximal eigenstate coefficient $\max_{\underline{\sigma}^z} |\langle \underline{\sigma}^z | E\rangle|^2 = |\langle \underline{\sigma}_0^z | E\rangle|^2$. The overbar indicates the average over disorder and a few mid-spectrum eigenstates.

Compared to the IPR_q, $\Pi(x)$ gives more information and is a good probe of the eigenstate's local structure in the Fock space. In particular, we can study the spread of $\Pi(x)$ by defining the moments

$$\overline{X^n} = \sum_x x^n \Pi(x), \tag{9}$$

and the mean-square displacement of it

$$\Delta X^2 = \overline{X^2} - \overline{X}^2. \tag{10}$$

In the ergodic phase, the infinite-temperature wave function is spread homogeneously on the Fock space and $\Pi^{\rm Erg.}(x)$ is given by a binomial distribution,

$$\Pi_p(L, x) = \binom{L}{x} (1-p)^{L-x} p^x \ , \tag{11}$$

with $p = 1/2$ and therefore $\overline{X} = L/2$ and $\Delta X^2 = L/4$. In the opposite limit of a strongly localized system, which can be approximated by the noninteracting case ($V = 0$), $\Pi(x)$ is still given by the binomial probability distribution Eq. (11), however the value of $p = \overline{\sin^2(\theta_i/2)}$ now strongly depends on the disorder W as

$$p = \frac{1}{2} - \frac{\overline{|h_i|}}{2\sqrt{1+h_i^2}} = \frac{1}{2} - \frac{\sqrt{W^2+1} - 1}{2W}. \tag{12}$$

As expected, $p \simeq 1/2 - W/4 \to 1/2$ as $W \to 0$ like in the ergodic phase, but for $V = 0$ it happens due to the system localization in σ^x basis, and $p \simeq 1/(2W) \to 0$ in the opposite limit of $W \to \infty$.

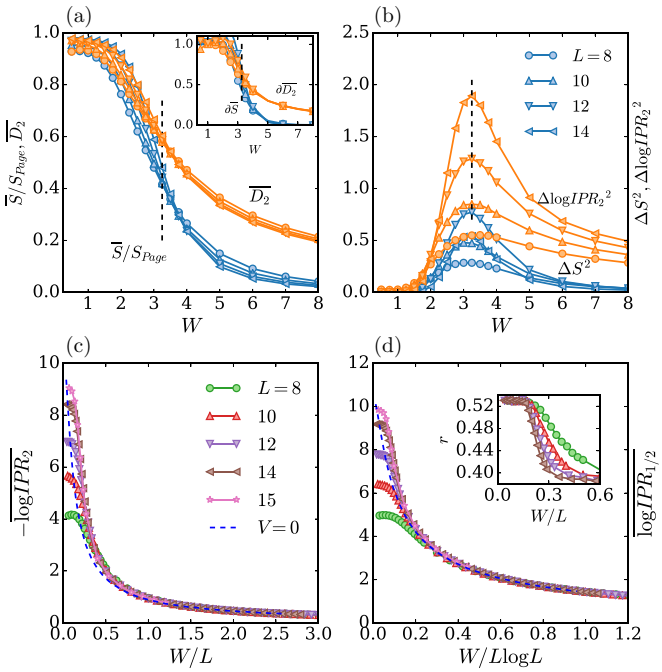

FIG. 2. (a) The averaged bipartite entanglement entropy rescaled by the Page value $S/S_{\rm Page}$ (blue) and the averaged fractal dimension D_2 (orange) versus the disorder strength W for $\widehat{H}_{\rm MBL}$. Inset shows the discrete derivatives of the entanglement entropy $\overline{\partial S} = 2(S(L) - S(L'))/(L - L')\log 2$ [53] (blue) and $\overline{\partial D_2} = -\log(\mathrm{IPR}_2(L)/\mathrm{IPR}_2(L'))/(L - L')\log 2$ (orange) with respect to the system size L. (b) Variances of the entanglement entropy S (blue) and of the $-\log \mathrm{IPR}_2$ (orange) versus W. In both panels the vertical dashed black line is a guide for eyes indicating the MBL transition. Symbols shown in panel (b) correspond to different system sizes. Next panels show disorder dependence of $-\overline{\log \mathrm{IPR}_q}$ for (c) $q = 2$ and (d) $q = 1/2$ with the correspondingly rescaled W according to the noninteracting limit (15). In both panels, the dashed blue line show the corresponding noninteracting case $V = 0$. The inset in (d) shows the ratio r statistics of the level spacings versus the rescaled W.

Note that in the limit $L \to \infty$ and in case pL, $(1-p)L \to \infty$ the binomial probability distribution in Eq. (11) can be approximated by a Gaussian distribution with mean and the variance given by

$$\overline{X} = pL\,, \quad \Delta X^2 = p(1-p)L\,. \tag{13}$$

III. RESULTS

In order to relate the ergodicity properties of the considered system with the local structure of its eigenstates in the Fock space, we focus on the behavior of the radial probability distribution $\Pi(x)$ of mid-spectrum eigenstates of $\widehat{H}_{\rm MBL}$. However, for sake of completeness we start our analysis by investigating some standard MBL indicators, which quantify ergodicity in the real and Fock space, such as bipartite entanglement entropy and IPR_q and compare their properties.

The entanglement entropy has been found to be a surrounding resource to test and quantify ergodicity in a system.

Figure 2(a) shows the half-chain bipartite entanglement entropy $S = -\mathrm{Tr}[\rho_{L/2}\log\rho_{L/2}]$ (blue lines) of the reduced density matrix $\rho_{L/2}$ of a mid-spectrum eigenstates of $\widehat{H}_{\rm MBL}$. As expected, at weak disorder S shows the volume law, $S \sim L$, and flows towards the Page value $S_{\rm Page} = L/2\log 2 - 1/2$ [36], which is the value for states randomly drawn in Fock space.

Instead, at strong disorder S has an area-law scaling, $S \sim O(1)$, and thus $S/S_{\rm Page} \sim 1/L$ tends to zero. The crossover between the two behaviors occurring at $W_c \approx 3.5$ indicates the MBL transition.

The averaged fractal dimension $\overline{D_2}$ in Eq. (5) is also shown in Fig. 2(a) (orange lines) and its behavior is consistent with the one of S. In the ergodic phase $\overline{D_2} \approx 1$, while for $W > W_c$ the fractal dimension converges with L to a value, which is strictly smaller than one ($\overline{D_2} < 1$).

A few comments are in order: The finite-size flow of $\overline{S}/S_{\rm Page}$ and $\overline{D_2}$ to unity with the increasing system size within the ergodic phase and the stability in the localized phase. The discrete derivatives $\overline{\partial S} = 2(S(L) - S(L'))/(L - L')\log 2$ [53] and $\overline{\partial D_2} = -\log(\mathrm{IPR}_2(L)/\mathrm{IPR}_2(L'))/(L - L')\log 2$ in the inset of Fig. 2(a) tend to converge to discontinuous functions of W with increasing L, with zero value of $\overline{\partial S}$ and strictly positive value of $\overline{\partial D_2}$ in the MBL phase. In addition, as clearly seen from Fig. 2(a), both $\overline{S}/S_{\rm Page}$ and $\overline{D_2}$ deviate from their ergodic values at the same disorder amplitude. At the critical point the variance of the entanglement entropy ΔS^2, which has been shown to be a useful probe for the transition [17,19], diverges with L [blue lines in Fig. 2(b)]. In analogy with S, we also inspect the variance of $-\log \mathrm{IPR}_2 = LD_2\log 2$, which also diverges around the critical point [orange lines in Fig. 2(b)].

The above observations give an indication of the following scenario. The upper bound for the unaveraged $S \leqslant D_1 L\log 2$ derived in [44] and the deviation of $\overline{S}$ from its ergodic Page-value limit $\overline{S} = S_{\rm Page}$ at the same W as $\overline{D_2}$, is consistent with the jump in $\overline{D_q}$ across the MBL transition from unity in the ergodic phase to a certain positive value $D_q < 1/2$ in the MBL phase. Moreover, the divergent fluctuations of D_q might lead to the saturation of the above bound [44] at the transition pushing $\overline{S}$ to undergo the volume-to-area–law scaling transition and $\overline{D_q}$ to experience a jump.

A. Fluctuations of the fractal dimension

To obtain more insights in Fig. 3 we analyze the behavior of the fractal dimension fluctuations via the probability distribution of D_2 for several relevant values of W.

Deeply in the ergodic phase D_2 tends to unity and its fluctuations are exponentially suppressed with L, as dictated by ETH at infinite temperature ([Figs. 3(a) and (b)]. Instead, in the localized phase [Fig. 3(d)], we expect $\overline{D_2} < 1/2$ and self-averaging in the sense that ΔD_2^2 goes to zero with increasing L. For the whole interval of W the variance is shown in the inset of Fig. 3(a) and it demonstrates this decay away the critical region $3 \lesssim W \lesssim 4$. The self-averaging of D_q in the MBL phase can be understood in its noninteracting limit ($V = 0$), where the variance decay as the inverse of the system size:

$$\Delta D_q^2 = \frac{\sum_i \Delta(\log \mathrm{IPR}_q^{(i)})^2}{L^2(1-q)^2\log^2 2} \sim \frac{1}{L}\,. \tag{14}$$

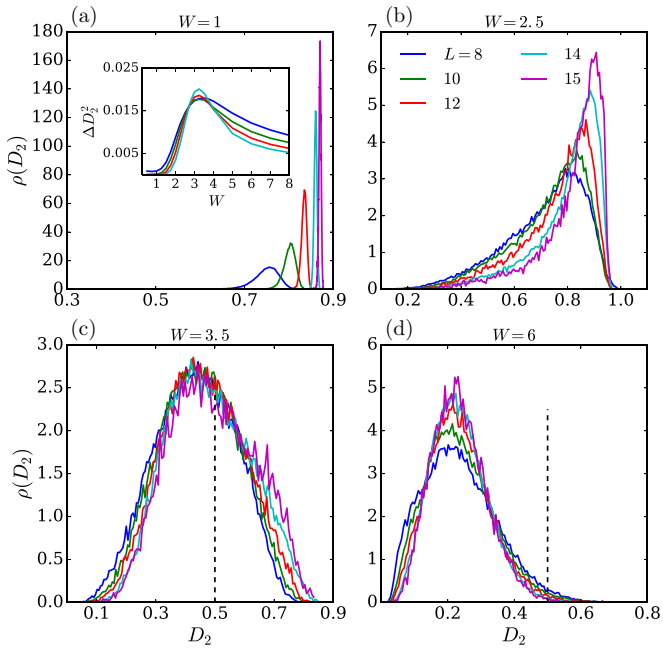

FIG. 3. Probability distribution function ρ of the fractal dimension D_2 for different disorder strength (a) $W = 1$, (b) $W = 2.5$, (c) $W = 3.25$, and (d) $W = 6$. Different colors represent system sizes L shown in the legend of panel (b). The inset shows the variance of the fractal dimension versus W establishing the nonself averaging property close to the MBL transition [$\Delta D_2^2 \sim O(L^0)$]. The vertical black dashed line in (c) and (d) indicate the value $D_2 = 1/2$.

On the contrary, in the critical region ($W \approx W_c$), we find that D_q is not self-averaging since its fluctuation does not decay with L [inset of Fig. 3(a)] and the probability distribution is stuck and not shrinking with increasing L [Fig. 3(c)].

At critical points of single-particle problems, self-averaging is usually absent if D_q demonstrates a jump [35]. Its absence is far from being trivial in many-body problems and it provides another case for the jump of D_q at the critical point. Summarizing, at the MBL transition D_q might be characterized by a jump and it is not self-averaging. This nonself-averaging and the relation between D_q and S [44] might drive the simultaneous jump-like transitions in $\overline{S}$ and $\overline{D_q}$.

It is important to point out once again that D_q is strictly positive due to the many-body nature of the problem. As a consequence, the MBL transition cannot been considered as an Anderson-localization transition in the Fock space with $D_q = 0$ in the localized phase, but rather as a transition between an ergodic ($D_q = 1$) and a nonergodic extended ($0 < D_q < 1$) phase. In order to reach a genuine localization transition in the Fock space one needs to rescale the disorder strength with L. Naively, as a first approximation, one might replace the Fock space on-site energies with independent distributed random variables with typical fluctuation $\sim\sqrt{L}$ as is done for the QREM [54–58]. If this would be the case, the Anderson transition would occur at $W_{AT} \sim \sqrt{L}\log L$ also for the quantum Ising model Eq. (1). Nevertheless, the Fock space on-site energies are strongly correlated and they cannot be approximated as independent random variables. Due to the presence of these correlations (similar to [59]) we expect that stronger disorder is needed to localize many-body states in the Fock space.

In order to understand the correct scaling of W_{AT} with L, we rely on the exactly solvable noninteracting case ($cV = 0$) providing the lower bound for D_q and then check numerically if the same scaling works as well at strong disorder in the interacting case. This comparison is motivated by the belief [45] that interacting eigenstates in the MBL phase are adiabatically connected to the ones of a noninteracting problem. Consequently, we expect to rescale W with L in *the same way* as in the noninteracting problem in order to have a genuine localization in the Fock space. Straightforward calculations of the single-spin $\mathrm{IPR}_q^{(i)} = \sin^4\frac{\theta_i}{2} + \cos^4\frac{\theta_i}{2}$ in the noninteracting model show that at large disorder W

$$\overline{D_q^0} \sim \begin{cases} W^{-2q} & q < 1/2, \\ \frac{\log W}{W} & q = 1/2, \\ W^{-1} & q > 1/2. \end{cases} \tag{15}$$

Thus rescaling $W \sim L$, we have $\mathrm{IPR}_q \sim O(1)$ for $q > 1/2$ and the system exhibits localization in the Fock space. In Fig. 2(c) we plot $-\overline{\log \mathrm{IPR}_2}$ for $V = 1$, which is collapsed after the rescaling W/L in agreement with the prediction of the noninteracting calculation.

The last observation should be compared to the scaling of W for the QREM, where $W_{\mathrm{QREM}} \sim \sqrt{L}\log L \ll L$ and the random many-body energies are uncorrelated. However, due to the limitation of system sizes achievable with exact diagonalization techniques, it is important to notice that a reasonable collapse of the curves in Fig 2(c) can also be obtained by rescaling $W/(\sqrt{L}\log L)$. Thus, in order to draw a distinction between the two scalings, we consider another moment $q = 1/2$ for IPR_q. The critical value for the QREM is independent of q, while for the MBL model we expect a different scaling with L for $q \leqslant 1/2$, as shown in Eq. (15). Figure 2(d) clearly demonstrates the collapse of $\overline{\log \mathrm{IPR}_{1/2}}$ for several L, by rescaling W with $L\log L$ in complete agreement with the prediction of Eq. (15).

Recently, some works [60–62] claim that the critical point for the MBL transition is L dependent and shifts as $W_c \sim L$. These claims are in conflict with our results for which the system is already Anderson-localized in the Fock space ($D_q = 0$) provided $W \sim L$. Localization in the Fock space is a much stronger breaking of ergodicity than the one defined using local observables (ETH). Since we expect to have $D_q = 1$ in a putative ergodic phase at infinite temperature, it implies that the critical point of the MBL transition, if it scales with system size, would have to scale slower than L ($W_c/L \to 0$), which rules out the prediction in Ref. [60–62].

Furthermore, we can argue a more strict bound on the possible behavior of W_c with L (if any), by comparing $\widehat{H}_{\mathrm{MBL}}$ with a proper constructed QREM. As we discussed, our model can be seen as an Anderson model on a hypercube with 2^L sites and correlated random on-site energies given by $E_{\sigma^z} = \sum_i h_i\sigma_i^z + \sum_i J_i\sigma_i^z\sigma_{i+1}^z$. Statistically, E_{σ^z}'s have zero mean and variance $\Delta E_{\sigma^z}^2(W) \sim L$. As first approximation one replaces the E_{σ^z} with Gaussian random variables with zero mean and variance $\Delta E_{\sigma^z}^2(W)$ (see, e.g., [63]). Doing so, we

have constructed a map between the original model $\widehat{H}_{\rm MBL}$ and the QREM, which is one to one.

From this perspective, the uncorrelated on-site disorder in QREM can be expressed in terms of strings of $\widehat{\sigma}^z$ operators

$$\sum_{\underline{\sigma}^z}^{2^L} E_{\underline{\sigma}^z} |\underline{\sigma}^z\rangle \langle\underline{\sigma}^z| = \sum_{k}^{L} \sum_{i_1,..,i_k} J^{(k)}_{i_1,...,i_k} \widehat{\sigma}^z_{i_1} \cdots \widehat{\sigma}^z_{i_k}, \tag{16}$$

with $J^{(k)}_{i_1,...,i_k} = \frac{1}{2^L} \sum_{\underline{\sigma}_z} E_{\underline{\sigma}^z} \sigma^z_{i_1} \cdots \sigma^z_{i_k}$ with $E_{\underline{\sigma}^z} \sim \mathcal{N}(0, \Delta E^2_{\sigma^z}(W))$.

As compared to the Hamiltonian $\widehat{H}_{\rm MBL}$, the constructed QREM contains longer range interactions, which will strongly break the integrability of the model. It is natural to expect that for a fix W the QREM will show an higher degree of ergodicity compared with $\widehat{H}_{\rm MBL}$, i.e., $r_{\rm MBL}(W) \leqslant r_{\rm QREM}(W)$. As a result, we expect the following concatenate inequalities [64]

$$W_c \leqslant W_{\rm QREM} \sim \sqrt{L} \log L < W_{AT} \sim L \tag{17}$$

imposing even stronger upper bound on the possible scaling of the MBL transition with L, which is not consistent with [60,61].

B. Radial probability distribution $\Pi(x)$

In this section, we show that the radial probability distribution $\Pi(x)$ in Eq. (8) of mid-spectrum eigenstate coefficients of $\widehat{H}_{\rm MBL}$ in the Fock space gives more detailed information on the wave function's local structure in the Fock space compared to IPR$_q$. In addition, it can be related to the local integrals of motion of $\widehat{H}_{\rm MBL}$ [14–16,45].

We recall that at strong disorder, deep in the MBL phase, the eigenstates $\{|E\rangle\}$ of $\widehat{H}_{\rm MBL}$ are believed to be adiabatically connected to the noninteracting ones $\{|\underline{\sigma}^z\rangle\}$ through a sequence of quasilocal unitary operators,

$$|E\rangle = \widehat{U} \, |\underline{\sigma}^z_0\rangle \, , \tag{18}$$

defining the integrals of motions $\widehat{\tau}^z_i = \widehat{U} \widehat{\sigma}^z_i \widehat{U}^\dagger$ for which $[\widehat{H}, \widehat{\tau}^z_i] = 0$.

Now, we use the above assumption to find the relation between the spread of the local integrals of motion $\{\widehat{\tau}^z_i\}$ and the moments of the probability distribution $\Pi(x)$. The Hamming distance between two Fock-states $|\underline{\sigma}^z\rangle$ and $|\underline{\sigma}^z_0\rangle$ is given by

$$d(\underline{\sigma}^z_0, \underline{\sigma}^z) = \sum_i \frac{(\sigma^z_i - \sigma^z_{0,i})^2}{4}, \tag{19}$$

where $\sigma^z_i = \langle\underline{\sigma}^z|\widehat{\sigma}^z_i|\underline{\sigma}^z\rangle$. The first moment of $\Pi(x, E)$, Eq. (9), for a certain eigenstate at energy E is given by

$$X(E) = \sum_x x \Pi(x, E) = \sum_\sigma d(\underline{\sigma}^z, \underline{\sigma}^z_0) \left|\langle\underline{\sigma}^z|\widehat{U}|\underline{\sigma}^z_0\rangle\right|^2, \tag{20}$$

where we use $|E\rangle = U \, |\underline{\sigma}^z_0\rangle$. Thus,

$$\begin{aligned} X(E) &= \frac{L}{2} - \frac{1}{2} \sum_i \sum_{\underline{\sigma}^z} \sigma^z_i \sigma^z_{0,i} \langle\underline{\sigma}^z_0|\widehat{U}^\dagger|\underline{\sigma}^z\rangle\langle\underline{\sigma}^z|\widehat{U}|\underline{\sigma}^z_0\rangle \\ &= \frac{L}{2} - \frac{1}{2} \sum_i \langle E|\widehat{\sigma}^z_i \widehat{\tau}^z_i|E\rangle \, . \end{aligned} \tag{21}$$

Averaging over disorder and energies E, we obtain

$$\overline{X} = \frac{L}{2} - \frac{1}{2} \overline{\sum_i \langle E|\widehat{\sigma}^z_i \widehat{\tau}^z_i|E\rangle} \tag{22}$$

Similar calculations show that the variance in Eq. (10) of $\Pi(x, E)$, $\Delta X^2(E) = \overline{X^2}(E) - \overline{X(E)}^2$, is given by

$$\begin{aligned} \Delta X^2(E) = \frac{1}{4} \sum_{i,j} \overline{\langle E|\widehat{\sigma}^z_i \widehat{\sigma}^z_j \widehat{\tau}^z_i \widehat{\tau}^z_j|E\rangle} - \\ - \frac{1}{4} \left(\sum_i \overline{\langle E|\widehat{\sigma}^z_i \widehat{\tau}^z_i|E\rangle} \right)^2 . \end{aligned} \tag{23}$$

Thus, both first cumulants, $\overline{X}$ and ΔX^2, provide the measures of the distance between the local integrals of motion $\{\widehat{\tau}^z_i\}$ and the undressed operators $\{\widehat{\sigma}^z_i\}$. In particular, in the MBL phase we expect a perturbative expansion $\tau^z_i = a^\alpha_{i_1} \widehat{\sigma}^\alpha_{i_1} / \sqrt{\xi_{\rm loc}} + b^{\alpha\beta}_{i_1 i_2} \widehat{\sigma}^\alpha_{i_1} \widehat{\sigma}^\beta_{i_2} + \cdots$ [65], where $a^\alpha_{i_1} \sim e^{-|i-i_1|/\xi_{\rm loc}}$, $b^{\alpha\beta}_{i_1 i_2} \sim e^{-(|i-i_1|+|i-i_2|)/\xi_{\rm loc}}$ decay exponentially, with the localization length $\xi_{\rm loc}$ providing the measure of the τ^z_i operator spread, and Latin letters run over site indices and Greek ones are in $\{x, y, z\}$. The coefficient $1/\sqrt{\xi_{\rm loc}}$, with $a^\alpha_i \sim O(1)$, provides the normalization of the operator $(\tau^z_i)^2 = 1$. Thus, $\overline{X}$ gives the direct estimate for the localization length

$$\overline{X} \sim \frac{L}{2} \left(1 - \sqrt{\frac{\xi_{\rm min}}{\xi_{\rm loc}}} \right) , \tag{24}$$

where $\xi_{\rm min}$ is an unimportant constant standing for some typical value of overlap $(a^\alpha_i)^2$ of the operators τ^z_i and σ^z_i at the same site. The main idea behind this formula is that from the W dependence of $\overline{X}$ one can infer the one of the localization length $\xi_{\rm loc}(W)$ up to a prefactor.

Having elucidated the relation between the integrals of motion and the radial probability distribution, we now present the numerical results for $\Pi(x)$, $\overline{X}$, and ΔX^2. Figure 4(a) shows $\Pi(x)$ for fixed system size $L = 16$ and several disorder strengths. As expected, at weak disorder, $\Pi(x)$ is centered in the middle of the chain, $\overline{X} = L/2$, with fluctuations $\Delta X^2 = L/4$ as shown in Figs. 4(b) and 4(c). In this case the shape of $\Pi(x)$ is close to the one $\Pi^{\rm Erg}(x)$ of an ergodic system, Eq. (11) with $p = \frac{1}{2}$. To quantify better the deviations of $\Pi(x)$ from $\Pi^{\rm Erg}(x)$, we consider the Hellinger distance

$$H_g = \frac{1}{\sqrt{2}} \sqrt{\sum_x \left(\sqrt{\Pi(x)} - \sqrt{\Pi^{\rm Erg}(x)} \right)^2} \, , \tag{25}$$

which is one of the common measures to quantify the distance between two probability distributions. The inset in Fig. 4(a) shows H_g as a function of W. In agreement with the IPR$_q$ analysis, at weak disorder H_q tends to zero exponentially fast with L, since the system is ergodic in the Hilbert space. At strong disorder in the MBL phase, $\Pi(x)$ has a nonergodic shape and it is skewed to the left with respect to its maximum, meaning that $\overline{X} < L/2$, Fig. 4(a), and H_g flows slowly with L to its maximal value $H_g = 1$.

Both mean $\overline{X}/L$ and variance $\Delta X^2/L$ normalized by L in Figs. 4(b) and 4(c) demonstrate similar behavior to the fractal dimension D_q and the normalized entanglement

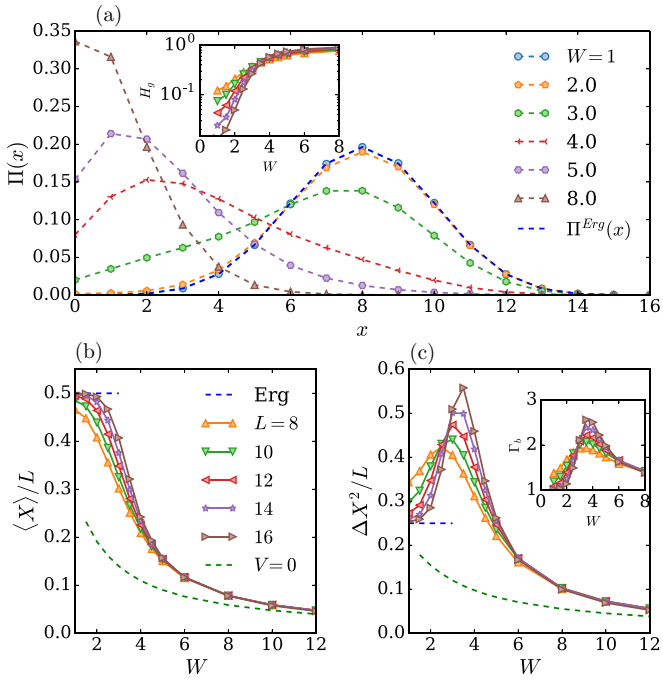

FIG. 4. (a) Radial probability distribution $\Pi(x)$ of the eigenstate coefficients in the Fock space, Eq. (8), for a fixed system size $L = 16$ and several disorder strengths W, ranging from the ergodic to the MBL phase (see legend). The blue dashed line show the ergodic prediction for $\Pi^{\rm Erg}(x) = \frac{1}{2^L}\binom{L}{L/2}$. Inset shows the Hellinger distance H_g, Eq. (25), between $\Pi(x)$ and the ergodic one $\Pi^{Erg}(x)$. (b) Mean $\overline{X}/L$, Eq. (9), and (c) variance $\Delta X^2/L$, Eq. (10), of $\Pi(x)$ as functions of W for several L. Symbol and color code is shown in legend. The blue and green dashed lines correspond to the ergodic and the noninteracting ($V = 0$) cases, respectively. The inset shows the deviation of $\Pi(x)$ from a binomial form (11) via the ratio $\Gamma_b = L\Delta X^2/\overline{X}(L-\overline{X})$.

entropy $\overline{S}/L$ and its fluctuations shown in Figs. 2(a) and 2(b). The quantity $\overline{X}/L$ decreases monotonically with W from its ergodic value (blue dashed line) toward the noninteracting one (green dashed curve). At $W \lesssim W_c$, $\overline{X}/L$ flows with L towards the ergodic value $\overline{X}/L = 1/2$, consistent with $\xi_{\rm loc}^{-1} = 0$ in Eq. (24). It shows the saturation with the system size in the MBL phase at the strictly positive value ($\xi_{\rm loc} > \xi_{\rm min}$). This behavior is consistent with the finite jump in $\xi_{\rm loc}^{-1}$ at the MBL transition. The deviations of $\overline{X}/L$ and $\Delta X^2/L$ in the MBL phase from their noninteracting limits and the saturation of these deviations with the system size are possibly related to the partial melting of the ergodic bubbles (initially ergodic active spins) in the avalanche scenario [28]. Indeed, our toy model takes into account the noninteracting ergodic spins, which are initially in resonance with each other and form the ergodic bubbles, while the presence of the interaction may make some the initially frozen spins to become active due to the hybridization with these bubbles.

Close to the transition $\Delta X^2/L$ exhibits a peak, which diverges with the system size, $\Delta X^2 \sim L^\alpha$, with $\alpha > 1$. The latter evidences a rather broad profile of $\Pi(x)$ going beyond the binomial approximation, Eq. (11). The inset to Fig. 4(c) emphasizes this by showing that the ratio $\Gamma_b = L\Delta X^2/\overline{X}(L-\overline{X})$ is strictly larger than its binomial unit value and demonstrates the same divergence with L as the variance $\Delta X^2/L$.

To sum up, in this section we have studied the radial probability distribution $\Pi(x)$, which is directly related to the local integrals of motions. In particular, the mean $\overline{X}$ of $\Pi(x)$ can be used to define a localization length $\xi_{\rm loc}$, Eq. (24). We have shown that at weak disorder $\overline{X} \to L/2$ corresponding to $\xi_{\rm loc} \to \infty$, while in the localized phase $0 < \overline{X}/L < 1/2$ giving finite $\xi_{\rm loc} > \xi_{\rm min}$. At the transition the fluctuations ΔX^2 diverge, which gives an evidence of a finite jump in $\overline{X}/L$ and therefore in $\xi_{\rm loc}^{-1}$ in the thermodynamic limit $L \to \infty$. The above finite jump in $\xi_{\rm loc}^{-1}$ is consistent with the avalanche theory of many-body delocalization [28] and therefore with the KT-type scaling of the transition [29,30].

In the next section, we consider a simple toy model of dilute ergodic "bubbles", which explains the observed phenomenon of the absence of D_q self-averaging, and helps us to bridge the gap between Fock space structure of mid-spectrum eigenstates, the avalanche theory, and the recent studies of phenomenological renormalization groups of MBL transition.

IV. DILUTE ERGODIC BUBBLES APPROXIMATION

In this section we discuss random block Hamiltonian consisting of noninteracting pieces, which is able to reproduce the numerical results described in the previous section. Reference [28] proposes that nonperturbative effects, such as rare thermal inclusions, which are unavoidable due to entropic arguments, can destabilize the MBL phase provided their density exceeds a certain critical value. As a consequence, an abrupt finite jump of the localization length is expected at the transition. Moreover, RG-studies [29,30] have shown that this avalanche theory should lead to a KT-like scaling behavior and the probability distribution $P(\ell)$ of the size ℓ of the largest thermal bubble has a power-law fat tail leading to a diverging variance.

With the aim to keep the toy model as simple as possible and avoid introducing further "fitting" parameters, we approximate the system in terms of only two species of spins, namely ρL active ergodic spins [66] and $(1-\rho)L$ noninteracting (frozen) spins. This approximation does not contain any partially frozen/nonergodically active spins for simplicity. As $\Pi(x)$ is not sensitive to the phases of the eigenstate's coefficients, and both ergodic and noninteracting limits of it are given by the binomial distribution in Eq. (11), we approximate the contributions of ergodic and frozen spins to the many-body wave function as the noninteracting ones [Eq. (2)], with $\overline{\sin^2\frac{\theta_i}{2}} = \frac{1}{2}$ for ρL active spins and $\sin\theta_i = 1/\sqrt{1+h_i^2}$ for the remaining $(1-\rho)L$ frozen ones, as they are subject to strong fields h_i. Due to self-averaging of the noninteracting contribution (14) we describe it by the mean value of p, Eq. (12). In this model, ρ plays the rote of the density of ergodic bubbles.

Within the above approximation, one can easily find $\Pi(x)$ as follows. At a spin-flip distance x from the eigenstate maximum we take k spin flips of *ergodic* type and $r-k$ of *frozen* type. The number of such paths from the maximal configuration point in the Fock space is given by

$$N_{k,x} = \binom{\rho L}{k}\binom{(1-\rho)L}{x-k}, \tag{26}$$

where the first combinatorial factor counts the number of possible selection of k indistinguishable spin-flips of the ergodic type out of ρL available ones, the second one counts the number of possible $r-k$ indistinguishable spin-flips of the frozen type out of $(1-\rho)L$ available ones. The corresponding wave function intensity averaged over h_i will be

$$|\psi_{k,x}|^2 = \left(\tfrac{1}{2}\right)^{\rho L} p^{x-k}(1-p)^{(1-\rho)L-x+k} . \tag{27}$$

The total number of selections for any k is given by

$$N_x = \sum_{k=0}^{x} N_{k,x} = \binom{L}{x} . \tag{28}$$

As a result, one can obtain the probability distribution $\Pi(x,\rho)$ at the fixed ergodic spin density ρ

$$\begin{aligned}\Pi(x,\rho) &= \sum_{k=0}^{x} N_{k,x}|\psi_{k,x}|^2 \\ &= \sum_{k=0}^{x} \Pi_{1/2}(\rho L,k)\Pi_p((1-\rho)L,x-k)\end{aligned} \tag{29}$$

which is simply given by the convolution of two binomial distributions

$$\Pi_{p'}(L',x') = \binom{L'}{x'} p'^{x'}(1-p')^{L'-x'} , \tag{30}$$

one describing the ergodic bubble ($p'=1/2$) and the other the remaining frozen spins with $p'=p<1/2$.

Due by the simple nature of the model, the IPR_q is the product of the IPR_qs for the ρL ergodic spins and the $(1-\rho)L$ frozen ones:

$$\begin{aligned}\mathrm{IPR}_q &= \sum_{x,k} N_{k,x}|\psi_{k,x}|^{2q} = \\ &= \left(\frac{1}{2}\right)^{(q-1)\rho L} [p^q+(1-p)^q]^{(1-\rho)L},\end{aligned} \tag{31}$$

and thus the fractal dimensions, Eq. (5), take the form

$$D_q(\rho) = \rho + (1-\rho)\overline{D_q^0} , \tag{32}$$

with $\overline{D_q^0}$ the fractal dimension of the noninteracting frozen spins, which is a continuous function of W with Eqs. (7) and (15). In this approximation any jump in the fractal dimension $D_q(\rho)$ is directly related to the jump in the bubble density ρ.

By using the Gaussian approximation Eq. (13) for the binomial distribution Eq. (11), we can estimate the first and second moment of $\Pi(x,\rho)$ in Eq. (29)

$$\overline{X}_\rho = \frac{L}{2} - \nu\varepsilon L, \tag{33}$$

$$\overline{X^2}_\rho = \left[\frac{L}{2} - \nu\varepsilon L\right]^2 + L\left[\frac{1}{4} - \nu\varepsilon^2\right], \tag{34}$$

and

$$\Delta X_\rho^2 = \overline{X^2}_\rho - \overline{X}_\rho^2 = L\left[\tfrac{1}{4} - \nu\varepsilon^2\right] , \tag{35}$$

where $\varepsilon = 1/2 - p$ and $\nu = 1-\rho \leqslant 1$. These results hold for fixed density ρ. For $\rho = 0$ and p given by (12), they coincide with the noninteracting results shown in Figs. 4(b) and 4(c) as green dashed lines, which show plots of Eqs. (33) and (35) for these parameters.

We emphasize that at any fixed ρ the ratio $\Gamma_b(\rho) = L\Delta X_\rho^2/\overline{X}_\rho(L-\overline{X}_\rho)$ is strictly smaller then its binomial value Γ_b in case $0<\nu<1$, $\varepsilon \neq 0$, which contradicts the numerics in the critical region [see the inset of Fig. 4(c)] as

$$\frac{\overline{X}_\rho}{L}\left(L-\overline{X}_\rho\right) = L\left[\frac{1}{4} - \nu^2\varepsilon^2\right] \tag{36}$$

is smaller than the one in Eq. (35). This observation underlines the importance of the fluctuations of ρ and the corresponding disorder average. Moreover, even the scaling of the maximum of $\Delta X^2 \sim L^\alpha$, $\alpha > 1$, from the exact numerics with L contradicts (35) with fixed ρ.

In order to recover the observed behavior of $\Gamma_b > 1$ in Fig. 4, it is crucial to take into account the nontrivial distribution $P(\rho)$ of the density of ergodic spins and perform the average over it. After averaging Eqs. (32), (33), and (34) and abbreviating

$$\int_0^1 \rho P(\rho)d\rho = \bar{\rho} \equiv 1-\bar{\nu}, \quad \int_0^1 \rho^2 P(\rho)d\rho - (\bar{\rho})^2 = \sigma_\rho^2, \tag{37}$$

one straightforwardly obtains

$$\bar{D}_q = 1 - \bar{\nu}(1-D_q^0) , \tag{38}$$

$$\overline{X} = \frac{L}{2} - \bar{\nu}\varepsilon L, \tag{39}$$

$$\Delta X^2 = \sigma_\rho^2\varepsilon^2 L^2 + L\left[\tfrac{1}{4} - \bar{\nu}\varepsilon^2\right] . \tag{40}$$

The properties of the probability distribution $P(\rho)$ of the density of ergodic spins can be extracted from the Refs. [27–30]. According to these works the distribution $P(\ell_i)$ of the length ℓ_i of a single ergodic bubble is (stretch)-exponential $P(\ell_i) \sim e^{-c\ell_i^d}$, or power law $P(\ell_i) \sim {\ell_i}^{-\alpha}$, $\alpha > 2$ in the MBL phase depending on its type. In the thermal phase, $P(\ell_i)$ is sharply concentrated on the length scale L of the system size and tends to a delta function for $L \to \infty$, meaning the entire system is ergodic. At the transition $P(\ell_i)$ is a power-law distributed $\sim \ell_i^{-\alpha_c}$ with the critical exponent $2 \leqslant \alpha_c \leqslant 3$ [28], in order to have finite mean $\overline{\ell} \sim L^0$ and diverging variance as $\overline{\ell^2} \sim L^{3-\alpha_c}$.

In our consideration we focus on the power-law probability distribution and determine the power α independently. Due to entropic reasons, the mean density $\overline{\rho}$ of the ergodic bubbles has to be finite even in the MBL phase. This density can be approximated by the sum of individual bubbles of lengths ℓ_i normalized by the system size

$$\rho \approx \sum_{i=1}^{K} \frac{\ell_i}{L} , \tag{41}$$

where K is a cut-off ensuring finite total length of order L of the chain. In the simplest approximation of independent identically distributed random ℓ_i one can apply the central limit theorem to ρ.

In the MBL phase where the mean and the variance of the length of a single ergodic bubble are finite, $\overline{\ell} \sim L^0$, $\overline{\ell^2} \sim L^0$,

i.e., $\alpha > 3$, and the number of bubbles scales as $K \sim L$ due to the boundness of $\overline{\rho} = K\overline{\ell}/L \sim L^0$, one obtains the Gaussian distribution of ρ with the variance decaying as

$$\sigma_\rho^2(W > W_c) = \bar{\rho^2} - \bar{\rho}^2 \sim \frac{1}{L}\,, \tag{42}$$

consistent with self-averaging. This also immediately confirms the self-averaging of D_q via Eq. (32). In a ergodic phase, the variance $\sigma_\rho(W < W_c)$ is exponentially small in L as $\overline{\rho} \to 1$. At the MBL transition self-averaging of ρ breaks down in this model only if $\overline{\ell^2} \to L^{3-\alpha_c}$ diverges in the thermodynamic limit, i.e., $\alpha_c < 3$. Due to the finite mean density

$$\overline{\rho} = \sum_{i=1}^{K} \frac{\overline{\ell_i}}{L} = \frac{K}{L} \max\left(L^0, L^{2-\alpha_c}\right) \sim L^0\,, \tag{43}$$

the number of ergodic bubbles scales as $K \sim \min(L, L^{\alpha_c - 1})$, which puts the lower bound on $\alpha_c > 1$. The corresponding scaling of the variance takes the form

$$\sigma_\rho^2(W \simeq W_c) \sim \min\left(L^0, L^{2-\alpha_c}\right),\ 1 < \alpha_c < 3\,. \tag{44}$$

The condition of ΔX^2 scaling faster than L is in agreement with the observations in Fig. 4(c), and requires $\alpha_c < 3$, which ultimately leads to the decay of the variance with L, but slower than L^{-1}. As a consequence, both in the MBL phase and at the transition the most significant contribution to ΔX^2 in (40) is given by the large fluctuations in ρ, cf. Eqs. (42) and (44).

The lack of self-averaging of D_q in Eq. (32) implies the more restrictive condition $\alpha_c \leqslant 2$. This is consistent with the finite mean $\overline{\ell} \sim L^0$ of a single bubble, $\alpha_c \geqslant 2$, only at the value $\alpha_c = 2$.

To summarize, in the ergodic phase $\rho = 1 - \nu$ goes to unity exponentially $\sim e^{-\eta L}$ and its variance has to decay also at least exponentially and therefore $\Delta X^2 (W \ll W_c) \simeq L/4$, as expected in the ergodic case. In the MBL phase $\overline{\rho}$ is finite and the variance decays as $1/L$ [cf. Eq. (42)], which yields a linear behavior of the mean $\overline{X} \sim L$ [cf. Eq. (39)], and the variance $\Delta X^2 \sim L$ [cf. Eq. (40)]. At the transition, $W = W_c$, according to Eq. (44), the variance of ρ is large compared to L^{-1} and, thus, it provides the main contribution to $\Delta X^2 \sim L^{4-\alpha_c} \gg L$, with $2 \leqslant \alpha_c \leqslant 3$, i.e.,

$$\Delta X^2/L \sim \begin{cases} 1/4 & W < W_c, \\ L^{3-\alpha_c} & W = W_c, \\ < 1/4 & W > W_c. \end{cases} \tag{45}$$

Finally, the constraint $\alpha_c = 2$ implies also that D_q is not self-averaging at the transition.

Thus, we have shown that our numerical results can be explained by considering a simple toy model of dilute ergodic bubbles embedded into a sea of frozen clusters. In particular, the divergence in $\Delta X^2/L$ requires to describe the probability distribution of the length of a typical ergodic bubble by a fat-tailed power-law distribution, which has diverge fluctuations at the transition,

$$\Delta D_q^2 \sim \sigma_\rho^2 \sim \begin{cases} e^{-\eta L} & W < W_c, \\ L^{2-\alpha_c} & W = W_c, \\ L^{-1} & W > W_c. \end{cases} \tag{46}$$

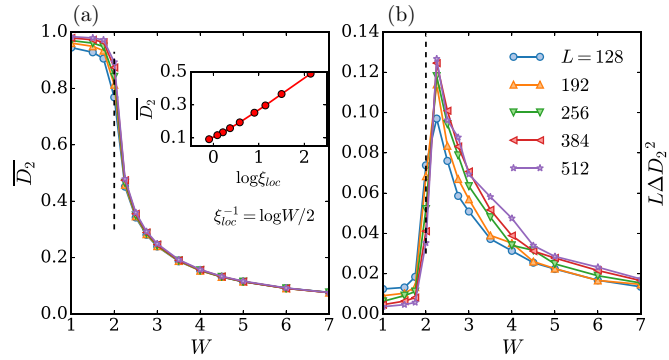

FIG. 5. (a) Fractal exponent D_2 and (b) its variance ΔD_2^2 for the noninteracting Aubry-André model with the many-body fermionic half-filling for several L vs the amplitude of the quasiperiodic potential W. The vertical black dashed line points to the critical point $W_c = 2$. The y axis of panel (b) has been rescaled to show that D_2 is self-averaging ($\Delta D_2^2 \sim 1/L$). The inset shows $\overline{D_2}$ for $W > 2$ as a function of the localization length $\xi_{\rm loc}^{-1} = \log W/2$.

V. CONTINUITY OF THE TRANSITION FOR NONINTERACTING SYSTEMS

In the previous sections, we have considered numerically the MBL transition from a Fock space perspective. We have shown that it is could be characterized by a finite jump in the fractal dimensions D_q, which are not self-averaging at the critical point. This scenario is consistent with the avalanche theory, which predict a KT-type scaling at the transition and therefore a finite jump on the inverse localization length $\xi_{\rm loc}^{-1}$. For a contrast, we now investigate the case in which the system undergoes a delocalization-localization transition with continuous $\xi_{\rm loc}^{-1}$, corresponding to the divergence of the localization length at the transition, $\lim_{W \to W_c} \xi_{\rm loc} \to \infty$. Concretely, we consider the noninteracting Aubrey-André model

$$\widehat{H}_{AA} = -\frac{1}{2} \sum_i \widehat{c}_{i+1}^\dagger \widehat{c}_i + h.c. + W \sum_i h_i \widehat{c}_i^\dagger \widehat{c}_i, \tag{47}$$

where $\widehat{c}_i^\dagger$ ($\widehat{c}_i$) is the fermionic creation (annihilation) operator at site i, $h_i = \cos(2\pi\beta i + \delta)$ is a quasiperiodic potential with $\beta = (\sqrt{5}+1)/2$, and δ is a random phase uniformly distributed in the interval $[0, 2\pi)$. This single-particle model is known to have an Anderson transition at $W_c = 2$ between extended ($W < 2$) and localized ($W > 2$) phases [67]. The single-particle localization length at transition diverges as $\xi_{\rm loc} \sim 1/\log W/2$. We consider noninteracting $\widehat{H}_{AA}$ with the many-body fermionic filling and focus on multifractal structure of the Slater-determinant many-body wave functions in the Fock space. For this reason, we take the model on L sites in the chain at half-filling $N = L/2$, where N is the number of particles, maximizing the Hilbert space dimension $\binom{L}{N} \sim 2^L/\sqrt{L}$. Fixing the basis of bare fermions $|\underline{n}\rangle = \prod_{n_i} (\widehat{c}_i^\dagger)^{n_i} |0\rangle$ as the computational basis, with $n_i \in \{0, 1\}$, we rewrite the model $\widehat{H}_{AA}$ in a similar form as Eq. (3) and investigate the ergodic properties of its eigenstates in the Fock space.

Figure 5(a) shows the fractal dimension $\overline{D_2}$ for the eigenstates of $\widehat{H}_{AA}$ constructed as a Slater determinant of taken at random N single-particle eigenstates. In the extended phase,

$W < 2$, the fractal dimension tends to unity, meaning that the typical eigenstate covers homogeneously the available Hilbert space. Instead, in the single-particle localized phase $W > 2$, $\overline{D_2}$ converges to a strictly positive value smaller than one. In fact, we expect that $\mathrm{IPR}_2 \sim (\frac{1}{\xi_{\mathrm{loc}}})^L$ similarly to a noninteracting spin chain Eq. (7), and as a consequence $D_2 \sim \log \xi_{\mathrm{loc}}$ close to the transition. Inset of Fig. 5(a) shows $\overline{D_2}$ as function $\log \xi_{\mathrm{loc}}$ giving an evidence of our prediction and therefore the many-body D_2 does not experience a jump across the transition. Another important consequence is that D_2 is self-averaging as shown in Fig. 5(b), $\Delta D_2^2 \sim 1/L$, everywhere including the transition. This self-averaging property should be compared to the one observed in the MBL model, for which the fractal dimensions are not self-averaging close to the MBL transition.

VI. CONCLUSIONS

In this paper we have studied the MBL transition of a chain of interacting spins from a Fock space point of view. In addition to the standard diagnostic tools for ergodicity such as fractal dimensions and entanglement entropy, we consider the radial probability distribution of eigenstate coefficients with respect to the Hamming distance in the Fock space from the wave function maximum. We show that this radial probability distribution gives important insights about the integrals of motion of the problem and allows to extract the localization length from the cumulants of the distribution.

Numerically we have found that both the fractal dimensions and the radial probability distribution have strong fluctuations at the critical point. The fractal dimensions at the transition are not self-averaging and the probability distribution is extremely broad. This divergence provides a rather strong evidence of the existence of a possible jump of the fractal dimensions as well as of the localization length across the MBL transition.

Inspired by recent studies of renormalization group and avalanche MBL theory, we explain our findings by introducing a simple spin toy model. This model hosts a finite density of ergodic/thermal bubbles as well as frozen/localized spins. The MBL transition occurs by tuning the density of the ergodic bubbles. At the transition the probability distribution of the bubble density is fat-tailed in agreement with the RG studies. Using this simple model, we are able to explain our numerical findings, and thus to bridge the gap between recent studies of the nature of the MBL transition in the "real space" and in the Fock space perspectives.

As a result, we show that the MBL transition can be seen as a transition between ergodic states to nonergodic extended states and we put an upper bound on the disorder scaling for a genuine Anderson localized regime with respect to the noninteracting case.

Finally, we provide an example of the many-body (noninteracting) model with a continuous localization transition showing the self-averaging of fractal dimensions in the whole range of parameters. This model confirms the conjectured relation between the nonself-averaging property of the fractal dimensions and their finite jump at the localization transition.

As the next steps in this direction it would be interesting to apply the developed tools to systems with few global constraints (like particle number conservation) or the driven systems undergoing the MBL transition in order to understand the similarities of the nonself-averaging nature of the fractal dimension and the moments of the radial distribution in such models. Another possible direction might be to provide the analytical arguments in favor of the scenario of the saturation of the bound [44] at the transition with the following jump in the fractal dimension to the value smaller than $D_q < 1/2$.

ACKNOWLEDGMENTS

We thanks D. Logan, A. Polkovnikov, S. Roy, and D. Sels for insightful discussions. G.D.T. acknowledges the hospitality of Max Planck Institute for the Physics of Complex Systems, Dresden, where part of the work was done. I.M.K. acknowledges the support of the Russian Science Foundation (Grant No. 21-12-00409). This work was partially supported by the DFG under EXC-2111–390814868. F.P. is funded by the European Research Council (ERC) under the European Unions Horizon 2020 Research and Innovation Program (Grant No. 771537) and under the DFG TRR80.

[1] J. M. Deutsch, Quantum statistical mechanics in a closed system, Phys. Rev. A **43**, 2046 (1991).

[2] M. Srednicki, Chaos and quantum thermalization, Phys. Rev. E **50**, 888 (1994).

[3] M. Srednicki, Thermal fluctuations in quantized chaotic systems, J. Phys. A **29**, L75 (1996).

[4] R. Marcos, D. Vanja, and O. Maxim, Thermalization and its mechanism for generic isolated quantum systems, Nature (London) **452**, 854 (2008).

[5] A. Polkovnikov, K. Sengupta, A. Silva, and M. Vengalattore, Colloquium: Nonequilibrium dynamics of closed interacting quantum systems, Rev. Mod. Phys. **83**, 863 (2011).

[6] L. D'Alessio, Y. Kafri, A. Polkovnikov, and M. Rigol, From quantum chaos and eigenstate thermalization to statistical mechanics and thermodynamics, Adv. Phys. **65**, 239 (2016).

[7] D. M. Basko, I. L. Aleiner, and B. L. Altshuler, Metal-insulator transition in a weakly interacting many-electron system with localized single-particle states, Ann. Phys. (NY) **321**, 1126 (2006).

[8] I. V. Gornyi, A. D. Mirlin, and D. G. Polyakov, Interacting Electrons in Disordered Wires: Anderson Localization and Low-T Transport, Phys. Rev. Lett. **95**, 206603 (2005).

[9] A. Pal and D. A. Huse, Many-body localization phase transition, Phys. Rev. B **82**, 174411 (2010).

[10] V. Oganesyan and D. A. Huse, Localization of interacting fermions at high temperature, Phys. Rev. B **75**, 155111 (2007).

[11] F. Alet and N. Laflorencie, Many-body localization: An introduction and selected topics, C. R. Phys. **19**, 498 (2018).

[12] R. Nandkishore and D. A. Huse, Many-body localization and thermalization in quantum statistical mechanics, Annu. Rev. Condens. Matter Phys. **6**, 15 (2015).

[13] D. A. Abanin, E. Altman, I. Bloch, and M. Serbyn, Colloquium: Many-body localization, thermalization, and entanglement, Rev. Mod. Phys. **91**, 021001 (2019).

[14] M. Serbyn, Z. Papić, and D. A. Abanin, Local Conservation Laws and the Structure of the Many-Body Localized States, Phys. Rev. Lett. **111**, 127201 (2013).

[15] D. A. Huse, R. Nandkishore, and V. Oganesyan, Phenomenology of certain many-body-localized systems, Phys. Rev. B **90**, 174202 (2014).

[16] V. Ros, M. Müller, and A. Scardicchio, Integrals of motion in the many-body localized phase, Nucl. Phys. B **891**, 420 (2015).

[17] D. J. Luitz, N. Laflorencie, and F. Alet, Many-body localization edge in the random-field Heisenberg chain, Phys. Rev. B **91**, 081103(R) (2015).

[18] E. Canovi, D. Rossini, R. Fazio, G. E. Santoro, and A. Silva, Quantum quenches, thermalization, and many-body localization, Phys. Rev. B **83**, 094431 (2011).

[19] J. A. Kjäll, J. H. Bardarson, and F. Pollmann, Many-Body Localization in a Disordered Quantum Ising Chain, Phys. Rev. Lett. **113**, 107204 (2014).

[20] G. De Tomasi, S. Bera, J. H. Bardarson, and F. Pollmann, Quantum Mutual Information as a Probe for Many-Body Localization, Phys. Rev. Lett. **118**, 016804 (2017).

[21] S. Vardhan, G. De Tomasi, M. Heyl, E. J. Heller, and F. Pollmann, Characterizing Time Irreversibility in Disordered Fermionic Systems by the Effect of Local Perturbations, Phys. Rev. Lett. **119**, 016802 (2017).

[22] I. V. Gornyi, A. D. Mirlin, and D. G. Polyakov, Many-body delocalization transition and relaxation in a quantum dot, Phys. Rev. B **93**, 125419 (2016).

[23] V. Khemani, S. P. Lim, D. N. Sheng, and D. A. Huse, Critical Properties of the Many-Body Localization Transition, Phys. Rev. X **7**, 021013 (2017).

[24] R. Vosk, D. A. Huse, and E. Altman, Theory of the Many-Body Localization Transition in One-Dimensional Systems, Phys. Rev. X **5**, 031032 (2015).

[25] S. Bera, H. Schomerus, F. Heidrich-Meisner, and J. H. Bardarson, Many-Body Localization Characterized from a One-Particle Perspective, Phys. Rev. Lett. **115**, 046603 (2015).

[26] A. Chandran, C. R. Laumann, and V. Oganesyan, Finite size scaling bounds on many-body localized phase transitions, arXiv:1509.04285.

[27] T. Thiery, M. Müller, and W. De Roeck, A microscopically motivated renormalization scheme for the MBL/ETH transition, arXiv:1711.09880.

[28] T. Thiery, F. Huveneers, M. Müller, and W. De Roeck, Many-Body Delocalization as a Quantum Avalanche, Phys. Rev. Lett. **121**, 140601 (2018).

[29] A. Goremykina, R. Vasseur, and M. Serbyn, Analytically Solvable Renormalization Group for the Many-Body Localization Transition, Phys. Rev. Lett. **122**, 040601 (2019).

[30] P. T. Dumitrescu, A. Goremykina, S. A. Parameswaran, M. Serbyn, and R. Vasseur, Kosterlitz-Thouless scaling at many-body localization phase transitions, Phys. Rev. B **99**, 094205 (2019).

[31] A. Morningstar and D. A. Huse, Renormalization-group study of the many-body localization transition in one dimension, Phys. Rev. B **99**, 224205 (2019).

[32] A. Morningstar, D. A. Huse, and J. Z. Imbrie, Many-body localization near the critical point, Phys. Rev. B **102**, 125134 (2020).

[33] B. L. Altshuler, Y. Gefen, A. Kamenev, and L. S. Levitov, Quasiparticle Lifetime in a Finite System: A Nonperturbative Approach, Phys. Rev. Lett. **78**, 2803 (1997).

[34] The main directions here can be characterized as the mapping of the MBL to the localization on hierarchical structures like a random regular graph (see, e.g., [68–86]), considerations of the spin models with uncorrelated on-site disorder like a Quantum Random energy model (see, e.g., [54–58,87] and some other ones [7,88–91]), as well as the associating of the MBL transition with the ergodic transition in random-matrix models [43,92–95].

[35] F. Evers and A. D. Mirlin, Anderson transitions, Rev. Mod. Phys. **80**, 1355 (2008).

[36] D. N. Page, Average Entropy of a Subsystem, Phys. Rev. Lett. **71**, 1291 (1993).

[37] However, there are several recent observations showing some significant deviations from complete randomness at the infinite temperature in a generic local non-integrable many-body system (see, e.g., [96–101] and references therein).

[38] A. De Luca and A. Scardicchio, Ergodicity breaking in a model showing many-body localization, Europhys. Lett. **101**, 37003 (2013).

[39] K. S. Tikhonov and A. D. Mirlin, Many-body localization transition with power-law interactions: Statistics of eigenstates, Phys. Rev. B **97**, 214205 (2018).

[40] N. Macé, F. Alet, and N. Laflorencie, Multifractal Scalings Across the Many-Body Localization Transition, Phys. Rev. Lett. **123**, 180601 (2019).

[41] N. Laflorencie, G. Lemarié, and N. Macé, Chain breaking and Kosterlitz-Thouless scaling at the many-body localization transition in the random-field Heisenberg spin chain, Phys. Rev. Research **2**, 042033(R) (2020).

[42] D. J. Luitz, I. M. Khaymovich, and Y. B. Lev, Multifractality and its role in anomalous transport in the disordered XXZ spin-chain, SciPost Phys. Core **2**, 6 (2020).

[43] M. Tarzia, Many-body localization transition in Hilbert space, Phys. Rev. B **102**, 014208 (2020).

[44] G. De Tomasi and I. M. Khaymovich, Multifractality Meets Entanglement: Relation for Nonergodic Extended States, Phys. Rev. Lett. **124**, 200602 (2020).

[45] J. Z. Imbrie, On many-body localization for quantum spin chains, J. Stat. Phys. **163**, 998 (2016).

[46] D. A. Abanin, J. H. Bardarson, G. De Tomasi, S. Gopalakrishnan, V. Khemani, S. A. Parameswaran, F. Pollmann, A. C. Potter, M. Serbyn, and R. Vasseur, Distinguishing localization from chaos: Challenges in finite-size systems, Ann. Phys. (NY) **427**, 168415 (2021).

[47] B. Derrida, Random-energy model: An exactly solvable model of disordered systems, Phys. Rev. B **24**, 2613 (1981).

[48] Y. Y. Goldschmidt, Solvable model of the quantum spin glass in a transverse field, Phys. Rev. B **41**, 4858 (1990).

[49] C. Manai and S. Warzel, Generalized random energy models in a transversal magnetic field: Free energy and phase diagrams, arXiv:2007.03290.

[50] M. Aizenman and S. Warzel, *Random Operators: Disorder Effects on Quantum Spectra and Dynamics* (American Mathematical Society, Providence, RI, 2015).

[51] E. J. Torres-Herrera, G. De Tomasi, M. Schiulaz, F. Pérez-Bernal, and L. F. Santos, Self-averaging in many-body quantum systems out of equilibrium: Approach to the localized phase, Phys. Rev. B **102**, 094310 (2020).

[52] The following properties hold $\Pi(x) \geqslant 0$ and $\sum_x \Pi(x) = 1$.

[53] The factor 2 in the discrete derivative ∂S of the entanglement entropy normalizes it to the ergodic value.

[54] C. R. Laumann, A. Pal, and A. Scardicchio, Many-Body Mobility Edge in a Mean-Field Quantum Spin Glass, Phys. Rev. Lett. **113**, 200405 (2014).

[55] C. L. Baldwin, C. R. Laumann, A. Pal, and A. Scardicchio, The many-body localized phase of the quantum random energy model, Phys. Rev. B **93**, 024202 (2016).

[56] L. Faoro, M. V. Feigelman, and L. Ioffe, Non-ergodic extended phase of the quantum random energy model, Ann. Phys. **409**, 167916 (2019).

[57] V. N. Smelyanskiy, K. Kechedzhi, S. Boixo, S. V. Isakov, H. Neven, and B. Altshuler, Nonergodic Delocalized States for Efficient Population Transfer within a Narrow Band of the Energy Landscape, Phys. Rev. X **10**, 011017 (2020).

[58] K. Kechedzhi, V. N. Smelyanskiy, J. R. McClean, V. S. Denchev, M. Mohseni, S. V. Isakov, S. Boixo, B. L. Altshuler, and H. Neven, Efficient population transfer via non-ergodic extended states in quantum spin glass, *13th Conference on the Theory of Quantum Computation, Communication and Cryptography (TQC 2018)*, Leibniz International Proceedings in Informatics (LIPIcs) (Schloss Dagstuhl–Leibniz-Zentrum fuer Informatik, Dagstuhl, Germany, 2018), pp. 9:1–9:16.

[59] S. Aubry and G. André, Analyticity breaking and Anderson localization in incommensurate lattices, Ann. Israel Phys. Soc. **3**, 18 (1980).

[60] J. Šuntajs, J. Bonča, T. Prosen, and L. Vidmar, Quantum chaos challenges many-body localization, Phys. Rev. E **102**, 062144 (2020).

[61] D. Sels and A. Polkovnikov, Dynamical obstruction to localization in a disordered spin chain, arXiv:2009.04501.

[62] T. LeBlond, D. Sels, A. Polkovnikov, and M. Rigol, Universality in the onset of quantum chaos in many-body systems, arXiv:2012.07849.

[63] S. Roy and D. E. Logan, Fock-space correlations and the origins of many-body localization, Phys. Rev. B **101**, 134202 (2020).

[64] Here we note that one can choose any model with longer range of interactions compared to the quantum Ising one (for example p-spin model) and provide an upper bound for the MBL transition. It appears that the QREM provides the most strict one, therefore here we have used it.

[65] Repeated indices are summed.

[66] Cf. the Supplemental Material of Ref. [40].

[67] A. Avila and S. Jitomirskaya, The Ten Martini Problem, Ann. Math. **170**, 303 (2009).

[68] G. Biroli, A. C. Ribeiro-Teixeira, and M. Tarzia, Difference between level statistics, ergodicity and localization transitions on the Bethe lattice, arXiv:1211.7334.

[69] A. De Luca, B. L. Altshuler, V. E. Kravtsov, and A. Scardicchio, Anderson Localization on the Bethe Lattice: Nonergodicity of Extended States, Phys. Rev. Lett. **113**, 046806 (2014).

[70] B. L. Altshuler, E. Cuevas, L. B. Ioffe, and V. E. Kravtsov, Nonergodic Phases in Strongly Disordered Random Regular Graphs, Phys. Rev. Lett. **117**, 156601 (2016).

[71] K. S. Tikhonov and A. D. Mirlin, Fractality of wave functions on a Cayley tree: Difference between tree and locally treelike graph without boundary, Phys. Rev. B **94**, 184203 (2016).

[72] K. S. Tikhonov, A. D. Mirlin, and M. A. Skvortsov, Anderson localization and ergodicity on random regular graphs, Phys. Rev. B **94**, 220203(R) (2016).

[73] G. Biroli and M. Tarzia, Delocalized glassy dynamics and many-body localization, Phys. Rev. B **96**, 201114(R) (2017).

[74] M. Sonner, K. S. Tikhonov, and A. D. Mirlin, Multifractality of wave functions on a Cayley tree: From root to leaves, Phys. Rev. B **96**, 214204 (2017).

[75] I. García-Mata, O. Giraud, B. Georgeot, J. Martin, R. Dubertrand, and G. Lemarié, Scaling Theory of the Anderson Transition in Random Graphs: Ergodicity and Universality, Phys. Rev. Lett. **118**, 166801 (2017).

[76] G. Biroli and M. Tarzia, Delocalization and ergodicity of the Anderson model on Bethe lattices, arXiv:1810.07545.

[77] V. E. Kravtsov, B. L. Altshuler, and L. B. Ioffe, Non-ergodic delocalized phase in Anderson model on Bethe lattice and regular graph, Ann. Phys. (NY) **389**, 148 (2018).

[78] G. Parisi, S. Pascazio, F. Pietracaprina, V. Ros, and A. Scardicchio, Anderson transition on the Bethe lattice: An approach with real energies, J. Phys. A **53**, 014003 (2019).

[79] S. Bera, G. De Tomasi, I. M. Khaymovich, and A. Scardicchio, Return probability for the Anderson model on the random regular graph, Phys. Rev. B **98**, 134205 (2018).

[80] G. De Tomasi, S. Bera, A. Scardicchio, and I. M. Khaymovich, Subdiffusion in the Anderson model on the random regular graph, Phys. Rev. B **101**, 100201(R) (2020).

[81] K. S. Tikhonov and A. D. Mirlin, Statistics of eigenstates near the localization transition on random regular graphs, Phys. Rev. B **99**, 024202 (2019).

[82] K. S. Tikhonov and A. D. Mirlin, Critical behavior at the localization transition on random regular graphs, Phys. Rev. B **99**, 214202 (2019).

[83] G. Biroli and M. Tarzia, Anomalous dynamics on the ergodic side of the many-body localization transition and the glassy phase of directed polymers in random media, Phys. Rev. B **102**, 064211 (2020).

[84] K. S. Tikhonov and A. D. Mirlin, Eigenstate correlations around many-body localization transition, Phys. Rev. B **103**, 064204 (2020).

[85] I. García-Mata, J. Martin, R. Dubertrand, O. Giraud, B. Georgeot, and G. Lemarié, Two critical localization lengths in the Anderson transition on random graphs, Phys. Rev. Research **2**, 012020(R) (2020).

[86] S. Roy and D. E. Logan, Localization on Certain Graphs with Strongly Correlated Disorder, Phys. Rev. Lett. **125**, 250402 (2020).

[87] G. Biroli, D. Facoetti, M. Schiroó, M. Tarzia, and P. Vivo, Out of equilibrium phase diagram of the quantum random energy model, Phys. Rev. B **103**, 014204 (2020).

[88] D. E. Logan and S. Welsh, Many-body localization in Fock space: A local perspective, Phys. Rev. B **99**, 045131 (2019).

[89] S. Roy, D. E. Logan, and J. T. Chalker, Exact solution of a percolation analog for the many-body localization transition, Phys. Rev. B **99**, 220201(R) (2019).

[90] S. Roy, J. T. Chalker, and D. E. Logan, Percolation in Fock space as a proxy for many-body localization, Phys. Rev. B **99**, 104206 (2019).

[91] G. De Tomasi, D. Hetterich, P. Sala, and F. Pollmann, Dynamics of strongly interacting systems: From Fock-space fragmentation to many-body localization, Phys. Rev. B **100**, 214313 (2019).

[92] V. E. Kravtsov, I. M. Khaymovich, E. Cuevas, and M. Amini, A random matrix model with localization and ergodic transitions, New J. Phys. **17**, 122002 (2015).

[93] V. E. Kravtsov, I. M. Khaymovich, B. L. Altshuler, and L. B. Ioffe, Localization transition on the random regular graph as an unstable tricritical point in a log-normal Rosenzweig-Porter random matrix ensemble, arXiv:2002.02979.

[94] I. M. Khaymovich, V. E. Kravtsov, B. L. Altshuler, and L. B. Ioffe, Fragile extended phases in the log-normal Rosenzweig-Porter model, Phys. Rev. Research **2**, 043346 (2020).

[95] I. M. Khaymovich and V. E. Kravtsov, Dynamical phases in a "multifractal" Rosenzweig-Porter model, arXiv:2106.01965.

[96] W. Beugeling, A. Andreanov, and M. Haque, Global characteristics of all eigenstates of local many-body Hamiltonians: Participation ratio and entanglement entropy, J. Stat. Mech.: Theory Exp. (2015) P02002.

[97] D. J. Luitz and Y. Bar Lev, Anomalous Thermalization in Ergodic Systems, Phys. Rev. Lett. **117**, 170404 (2016).

[98] W. Beugeling, A. Bäcker, R. Moessner, and M. Haque, Statistical properties of eigenstate amplitudes in complex quantum systems, Phys. Rev. E **98**, 022204 (2018).

[99] R. Hamazaki and M. Ueda, Atypicality of Most Few-Body Observables, Phys. Rev. Lett. **120**, 080603 (2018).

[100] A. Bäcker, M. Haque, and I. M Khaymovich, Multifractal dimensions for random matrices, chaotic quantum maps, and many-body systems, Phys. Rev. E **100**, 032117 (2019).

[101] M. Haque, P. A. McClarty, and I. M. Khaymovich, Entanglement of mid-spectrum eigenstates of chaotic many-body systems–deviation from random ensembles, arXiv:2008.12782.